J. Fluid Mech. (1996), vol. 327, pp. 325–341

Formation of a pointed drop in Taylor's four-roller mill

By LEONID K. ANTANOVSKII†

Department of Mathematics, Monash University, Clayton, Victoria 3168, Australia

(Received 5 March 1996 and in revised form 2 July 1996)

The paper addresses the mathematical modelling of the formation of a pointed drop in a four-roller mill, observed by Taylor (1934) in the Cavendish Laboratory. Since the experiments were carried out with drops of small diameter compared to the mill size, the method of matched asymptotic expansions is applicable. A two-dimensional Stokes flow generated by the rotating rollers in the mill but with no drop effect (outer problem) is computed numerically by a boundary-element method. The local expansion of that flow at the centre of the mill, where the drop is to be positioned, is used as a far field for the flow around the drop in unbounded fluid (inner problem). Employing a plane-flow model and using complex-variable techniques, the explicit solutions previously obtained by the author are adapted to the inner problem. It is proved that, with an increasing rotation rate of the rollers, the drop does develop two apparent cusps on the interface, and its shapes have striking similarities with Taylor's experiments. Response diagrams showing the drop distortion versus the elongational strain demonstrate that these are one-to-one function of each other if the drop diameter is greater than a critical value determined by the size of the mill but cease to be one-to-one otherwise. This behaviour is identified with a sudden transition from a rounded drop to a cusped one at a critical strain.

1. Introduction

Some experiments on deformation of viscous and inviscid drops subjected to extensional flow, at low Reynolds number, were described by Taylor (1934). In the experiments a neutrally buoyant single drop was placed in a four-roller mill filled with golden syrup, a highly viscous liquid, and then the effect of increasing flow velocity on the shape of the drop was observed. When the drop viscosity was not small compared with that of the exterior fluid, the drop was always rounded, and its elongation gradually increased with increasing rate of strain up to bursting. However, for inviscid drops, a sudden transition in shape at a critical straining rate was revealed, resulting in the abrupt formation of pointed ends. These experiments were then carefully repeated by Rumscheidt & Mason (1961), and many interesting phenomena were documented, including the existence of steady pointed drops, bursting rounded drops and even bursting pointed drops (see also the review by Stone 1994). Similar effects of the formation of a singularity in the free surface were observed by Moffatt (1977), Joseph *et al.* (1991) and Jeong & Moffatt (1992) in a number of free-surface flows induced by rotating cylinders.

† Present address: Moldflow International Pty Ltd, 259–261 Colchester Road, Kilsyth, Victoria 3137, Australia.

Concerning the mathematical modelling of the formation of a pointed drop, many difficulties were encountered, arising from the presence of the free surface that undergoes very large deformation and from the fact that the flow set up by Taylor is genuinely three-dimensional. Since the pointed drop is usually spindle-shaped but the far field is two-dimensional, two qualitative models naturally suggest themselves, which are based on the assumptions of either axisymmetric or plane flow. The behaviour of axisymmetric drops was studied numerically by Youngren & Acrivos (1976) employing a boundary-element method and by Buckmaster (1972, 1973), Acrivos & Lo (1978) and Sherwood (1981, 1984) using the assumption of a slender drop. Asymptotical analysis of the deformation of a three-dimensional droplet placed in Taylor's flow, was presented by Hinch & Acrivos (1979). Unfortunately, both numerical and asymptotical methods are unable to resolve fine details of the flow and the drop shape near the pointed ends. Thus, any analytical solution to the problem of the formation of a pointed drop is of great interest.

The first attempt at analytical investigation of the drop deformation was undertaken by Richardson (1968). Using complex-variable techniques, an elegant analysis of the deformation of a plane inviscid drop subjected to a pure straining flow with linear far field was implemented. The explicit solutions obtained showed that the drop always had an elliptical cross-section. Therefore, none of these solutions exhibits cusps or provides any evidence of bursting. Seemingly, this surprising result discouraged future researchers, since it was conjectured that the elliptical shape might be an intrinsic feature of the plane-flow model (Buckmaster 1973). Notwithstanding this, Richardson (1973) demonstrated that the shape of a plane inviscid drop placed in a parabolic (Poiseuille) flow has striking similarities with some experiments on three-dimensional bubbles introduced into a fluid flowing through a circular tube. This is a good reason to believe that the plane-flow model is capable of retaining the essential physics.

Moreover, Professor D. D. Joseph suggested in a private conversation at the 3rd Caribbean Congress on Fluid Dynamics (Caracas, Venezuela, February 1995) that the singularity is likely to be two-dimensional as in Liu, Liao & Joseph (1995), motivated by the plausible instability of axisymmetric pointed ends. If that is the case, the cusp should be in the plane of the rollers' axles and hence could not be observed from the front side of the mill. This is also confirmed by the experiments on the skirt formation on a fairly large bubble trying to squeeze between two counter-rotating cylinders in a highly viscous fluid, which were carried out by Professor H. K. Moffatt (1992, unpublished) in the two-roller apparatus described in Jeong & Moffatt (1992).

The approach of Richardson (1968) is extended in Antanovskii (1994*b*) to a two-dimensional time-evolving inviscid drop initially placed within a potential viscous flow. If the complex velocity of this flow behaves at infinity as a polynomial, a broad class of explicit time-dependent solutions is found, which incorporate those obtained by Richardson (1968) as the steady-state case, and are similar, in some respects, to explicit solutions describing the coalescence of a two-dimensional drop in vacuum deduced by Hopper (1990, 1991) and Richardson (1992), and extended to semi-infinite flow domains by Hopper (1992, 1993) and Jeong & Moffatt (1992). Recently, Tanveer & Vasconcelos (1995) demonstrated that these solutions are also relevant to time-evolving inviscid drops (bubbles) placed in a shear (rotational) flow with a linear velocity field at infinity.

A steady-state flow around a two-dimensional inviscid drop placed in fluid the velocity of which at large distances is that of a general Stokes flow with non-vanishing vorticity, was considered in Antanovskii (1994*c*). Again, if the far-field velocity is a polynomial, explicit solutions generalizing those derived by Richardson (1973), are

obtained. These solutions were applied to the modelling of the formation of a pointed drop in Antanovskii (1994c, 1995). In particular, it was demonstrated that a drop within a Stokes flow, being the superposition of pure straining (corner) flow with a linear velocity field and a motion described by cubic terms, no longer had an elliptical cross-section. Depending on the cubic terms, there are two mutually exclusive regimes of behaviour for the drop with increasing strain, which can be identified with the onset of either cusping or bursting. In the first case a drop survives for all attainable strains, developing very sharp ends, whereas in the second case there is an upper bound for strains at which a steady solution still exists. In addition, it is shown that the elongational strain is not monotonic with respect to the drop deformation as the cubic terms become smaller (Antanovskii 1995). The non-monotonic dependence can be identified with a sudden transition of the rounded ends of the drop to the pointed ones through instability and bifurcation. However, in the above papers nothing is said about the local structure of the real flow field in Taylor's mill, on which the drop behaviour appears to depend drastically.

In this paper a more realistic flow in Taylor's four-roller mill is considered. Following the spirit of matched asymptotic expansions, the velocity field undisturbed by the presence of the drop (outer problem) is computed numerically by means of a boundary-element method. An appropriately truncated Taylor series of this solution about the mill centre is then used as a far field for the flow around the drop (inner problem). This problem is solved analytically by means of complex-variable techniques. It is revealed that an inviscid drop positioned at the centre of the mill (being a stagnation point) is increasingly distorted by the flow, with two apparent cusps developing in the free surface. This is in complete agreement with Taylor's experiments. The response diagrams showing the drop deformation versus capillary number, the ratio of elongational strain to capillary forces, are plotted for some drop radii. It is demonstrated that the response diagrams show one-to-one function for a drop of radius greater than a critical value determined by the mill geometry but cease to be one-to-one otherwise. This fact describes a sudden transition in shape through instability of one of the multiple solutions.

All the numerical simulations are carried out exactly for Taylor's experiments described in detail in §2. An asymptotic mathematical model is formulated in §3, and the solution is presented in §4. The results obtained are discussed in §5.

2. Description of Taylor's experiments

To study the stirring processes in emulsions composed of two immiscible liquids, the four-roller mill sketched in figure 1 was designed by Taylor (1934). Four brass cylinders of length 3.81 cm and diameter 2.39 cm were mounted at the corners of a square of sides 3.18 cm. Their axles ran in brass bearings fixed in two glass plates which formed the sides of a box of internal dimensions $7.6 \times 7.6 \times 3.9$ cm. The remaining sides were brass. The box was filled with golden syrup (concentrated sugar solution) diluted with a small quantity of water till the viscosity μ was between 50 and 150 $\mathrm{g\,cm^{-1}\,s^{-1}}$.

The cylinders were driven in the directions indicated by arrows in figure 1 at the same speed to produce a flow which was locally the corner flow represented by

$$v_x = G\,x\,, \quad v_y = -G\,y\,, \quad p = \text{constant}\,, \tag{2.1}$$

where (x, y) are the Cartesian coordinates as shown in figure 1, (v_x, v_y) are the

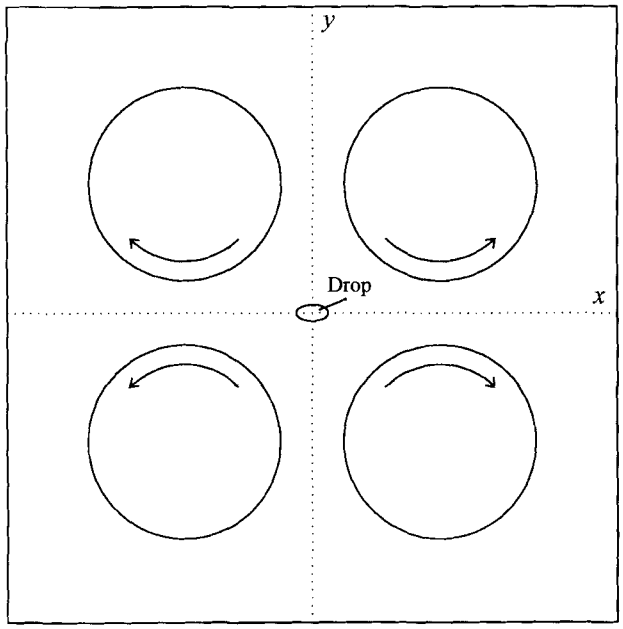

FIGURE 1. Schematic of Taylor's four-roller mill.

corresponding components of velocity, and p is the pressure. The stream lines of this flow are rectangular hyperbolas.

It is conceivable that $G = C_0/T$ at low Reynolds number, where T is the time of one revolution of the cylinders, and C_0 is a dimensionless constant of the apparatus. To measure C_0, the times taken for images of small particles in the golden syrup to pass along the x-axis (from x_1 to x_2) were observed, as well as the time T. Using equation (2.1), the deformation rate is given by

$$G = \frac{\log(x_2/x_1)}{t_2 - t_1}.$$

The times taken to cover 0.5 cm segments were measured for a particular $T = 48.7$ s, which suggested that $G = 0.105\ \mathrm{s}^{-1}$ and hence $C_0 = 5.1$ (see columns 1–3 of table 1 in §5).

A number of liquids of viscosity μ' which do not mix with water were used for the drop placed at the centre of the mill. For low values of the viscosity ratio μ'/μ (which are of interest here), a mixture of carbon tetrachloride with the paraffin oil was made up to be of the same density as the syrup. In this case, $\mu' = 0.034\ \mathrm{g\,cm^{-1}\,s^{-1}}$ and hence μ'/μ was sufficiently small to treat the drop liquid as inviscid. The interfacial surface tension between the two liquids was measured as $\sigma = 23\ \mathrm{dyn\,cm^{-1}}$.

Before setting the apparatus in motion, the drop was introduced into the syrup, and it became spherical under the influence of surface tension and was photographed in that condition in order to measure its radius R. In Taylor's experiments, the drop radius was in the range 0.12 to 0.25 cm. The apparatus was then set in motion at a slow speed and adjusted till the drop was steady and stationary, and a photograph was then taken. This procedure was repeated for an increased speed of motion, and

a sequence of photographs was obtained from which the deformation parameter,

$$\delta = \frac{R_{max} - R_{min}}{R_{max} + R_{min}}, \tag{2.2}$$

was calculated. Here R_{max} and R_{min} are the major and minor axes of the distorted drop in the (x, y)-plane, respectively. The capillary number,

$$\lambda = \frac{2\mu G R}{\sigma}, \tag{2.3}$$

being the ratio of disruptive elongational stresses to cohesive capillary forces, was simultaneously measured, and the response diagram (λ, δ) was then plotted.

At a low rotation rate of the cylinders, the drop was observed to be only slightly distorted from the spherical form, and the response diagram satisfied nearly exactly the condition $\delta = \lambda$, which was in excellent agreement with the theory previously formulated by Taylor (1932). For a higher rotation rate of the cylinders, the drop developed into a form which was far from spherical, and at a critical rate $\lambda = 0.41$ the drop ends suddenly became pointed. Actually, the drop being fairly large ($R = 0.25$ cm), it was not in a truly steady state, for after developing the pointed ends a thin skin appeared to slip off its surface, and the drop again became rounded. This configuration persisted and the ends of the resulting smaller drop ($R = 0.12$ cm) again became pointed at $\lambda = 0.65$. Further increases in strain merely increased the drop elongation, and the pointed configuration survived up to considerably higher strains ($\lambda = 2.45$) with no sign that the drop would burst.

3. The mathematical model

Consider an inviscid drop placed within a four-roller mill filled with a highly viscous liquid of the same density (see figure 1). In particular, the drop is neutrally buoyant in the exterior fluid, and hence gravity is completely removed from our analysis. In order to model the experiments in a qualitative fashion, a two-dimensional problem is considered throughout, which will enable us to use explicit solutions via employing complex-variable techniques and conformal mappings.

Let $\mathscr{D}$ be the two-dimensional flow domain 'occupied' by the exterior fluid (golden syrup), which is bounded by the rigid walls $\mathscr{B}$ of the mill and the rollers, and by the drop interface $\mathscr{S}$. The curve $\mathscr{S}$ encloses the drop $\mathscr{D}'$. Since the golden syrup is of very high viscosity μ, the flow velocity $\boldsymbol{v}$ and pressure p are governed by the Stokes equations

$$\nabla \cdot \boldsymbol{v} = 0, \quad \nabla p = \mu \Delta \boldsymbol{v} \quad \text{in } \mathscr{D}. \tag{3.1}$$

Insofar as the drop viscosity $\mu' \ll \mu$, it may be assumed that the velocity field in $\mathscr{D}'$ vanishes and hence the drop pressure p' is constant. Since a constant pressure superposed on the whole flow field does not alter the dynamics of an incompressible drop, one can put $p' = 0$ without loss of generality.

The flow velocity vanishes at the mill walls and is given at the rollers' surface. This kinematic condition reads

$$\boldsymbol{v} = \boldsymbol{V} \quad \text{on } \mathscr{B}, \tag{3.2}$$

where $\boldsymbol{V}$ is the given tangential velocity of the rigid boundary ($\boldsymbol{V} = 0$ on the mill walls). Furthermore, the kinematical free-surface condition and the dynamic (force balance) condition are imposed on the free boundary,

$$\boldsymbol{v} \cdot \boldsymbol{n} = 0, \quad p\boldsymbol{n} - \mu (\boldsymbol{n} \cdot \nabla \boldsymbol{v} + \nabla \boldsymbol{v} \cdot \boldsymbol{n}) = \sigma \kappa \boldsymbol{n} \quad \text{on } \mathscr{S}, \tag{3.3}$$

where $\boldsymbol{n}$ is a unit normal vector, κ the curvature of $\mathscr{S}$, and σ the surface tension. Note that the position of the free boundary $\mathscr{S}$ is unknown *a priori*. Finally, the drop area A is given.

3.1. *Asymptotic decomposition of the problem*

Since the drop diameter is assumed to be small compared with the size of the four-roller mill, the exterior flow field is only slightly disturbed by the presence of the drop. Therefore, to the first approximation, the outer solution is determined in the whole mill by equations (3.1) and (3.2). On the other hand, the drop itself experiences only slightly the presence of the rigid walls and hence is mainly driven by the local flow field, which will play the role of a far field for the flow around the drop in unbounded fluid (inner solution). This is the standard procedure of matched asymptotic expansions.

Thus, the outer solution $\boldsymbol{v}^\infty$ and p^∞ satisfies the problem

$$\nabla \cdot \boldsymbol{v}^\infty = 0\,, \quad \nabla p^\infty = \mu \Delta \boldsymbol{v}^\infty \quad \text{in } \mathscr{D}^\infty\,, \tag{3.4}$$

$$\boldsymbol{v}^\infty = \boldsymbol{V} \quad \text{on } \mathscr{B}\,, \tag{3.5}$$

where $\mathscr{D}^\infty$ is the region completely bounded by $\mathscr{B}$. Upon solving this well-posed problem, an appropriately truncated expansion of the velocity $\boldsymbol{v}^\infty(z)$ and pressure $p^\infty(z)$ about the stagnation point $z = 0$ is calculated, which will be denoted by $\boldsymbol{V}^\infty(z)$ and $P^\infty(z)$, respectively. Here $z = (x, y)$ is a position point. Then the inner solution $\boldsymbol{v}^\circ$ and p° is determined by the problem

$$\nabla \cdot \boldsymbol{v}^\circ = 0\,, \quad \nabla p^\circ = \mu \Delta \boldsymbol{v}^\circ \quad \text{in } \mathscr{D}^\circ\,, \tag{3.6}$$

$$\boldsymbol{v}^\circ \cdot \boldsymbol{n} = 0\,, \quad p^\circ \boldsymbol{n} - \mu\,(\boldsymbol{n} \cdot \nabla \boldsymbol{v}^\circ + \nabla \boldsymbol{v}^\circ \cdot \boldsymbol{n}) = \sigma \kappa \boldsymbol{n} \quad \text{on } \mathscr{S}\,, \tag{3.7}$$

$$\boldsymbol{v}^\circ \sim \boldsymbol{V}^\infty(z)\,, \quad p^\circ \sim P^\infty(z) \quad \text{as } |z| \to \infty\,, \tag{3.8}$$

where $\mathscr{D}^\circ$ is the complement of $\mathscr{D}'$ in the (x, y)-plane.

4. Solution of the problem

4.1. *Complex variables*

Let us first recall the complex representations for a two-dimensional Stokes flow (Langlois 1964). In the Cartesian (x, y)-plane this flow may be described in terms of the stress–stream function $w = \varphi + \mathrm{i}\psi$, which is a bi-analytic function of the complex variable $z = x + \mathrm{i}y$. The latter means that w satisfies the double Cauchy–Riemann equation

$$\frac{\partial^2 w}{\partial z^{*2}} = 0\,, \quad \frac{\partial}{\partial z^*} = \frac{1}{2}\left(\frac{\partial}{\partial x} + \mathrm{i}\frac{\partial}{\partial y}\right)\,,$$

which is equivalent to the Stokes equations (3.1). In particular, w can be expressed in terms of two analytic Goursat functions, say w_0 and w_1, as

$$w = w_0(z) + z^* w_1(z)\,. \tag{4.1}$$

Here and throughout this paper an asterisk is used to denote the complex conjugate.

The complex velocity field $v = v_x + \mathrm{i}v_y$, pressure p and stresses $F(\mathrm{d}z)$ exerted on an element $\mathrm{d}z$,

$$F(\mathrm{d}z) = \mathrm{i}\left(p\,\mathrm{d}z + 2\mu \frac{\partial v}{\partial z^*}\,\mathrm{d}z^*\right)\,,$$

are given by

$$v = \mathrm{i}\nabla\psi \ , \quad p = -\mu\Delta\varphi \ , \quad F(\mathrm{d}z) = -2\mu\,\mathrm{i}\,\mathrm{d}(\nabla\varphi) \ . \tag{4.2}$$

It is clear that ψ is the customary stream function, and φ is Airy's stress function.

Let s and n be the arclength and the inward normal coordinate at the boundary of the flow domain $\mathscr{D}$. It is assumed that the direction of s is selected in such a manner that the local coordinates (s,n) and the Cartesian co-ordinates (x,y) have the same orientation. In other words, the unit normal and tangent vectors have the relation

$$\frac{\partial z}{\partial n} = 1\,\frac{\partial z}{\partial s} \ .$$

This agreement is widely used in complex analysis.

In terms of the stress–stream function, the boundary conditions (3.2) and (3.3) take the form

$$\psi = 0 \ , \quad \frac{\partial\psi}{\partial n} = -V_s \quad \text{on } \mathscr{B} \ , \tag{4.3}$$

$$\psi = 0 \ , \quad \varphi = 0 \ , \quad 2\mu\frac{\partial\varphi}{\partial n} = \sigma \quad \text{on } \mathscr{S} \ , \tag{4.4}$$

where V_s is the tangential component of velocity (V_s is zero on the mill walls, but is constant on the rollers' boundary). The boundary conditions for φ follow from the dynamic condition written in the form

$$F(\mathrm{d}z) \equiv -2\mu\,\mathrm{i}\,\mathrm{d}(\nabla\varphi) = \mathrm{d}\left(\sigma\frac{\partial z}{\partial s}\right) \quad \text{on } \mathscr{S} \ ,$$

because

$$\frac{\partial^2 z}{\partial s^2} = \kappa\frac{\partial z}{\partial n}$$

due to Frenet's formula. The integration constants are omitted, since the stress–stream function w is defined by v and p apart from a linear function $\mathrm{Re}\,(a^* z) + b$, where a and b are complex constants.

Note that the flow is assumed to be symmetric about the x- and y-axes, and additionally with respect to rotation by the angle $\pi/2$. This is equivalent to the conditions

$$v\left(z^*\right)^* = v(z) \ , \quad -v(-z) = v(z) \ , \quad \mathrm{i}v(\mathrm{i}\,z) = v(z) \ . \tag{4.5}$$

Also, the drop shape is symmetric about the x- and y-axes.

4.2. *Outer solution*

The two-dimensional outer flow field is computed numerically by the boundary-element method (Hromadka II & Lai 1987; Pozrikidis 1992), which is here adapted to flows satisfying the symmetry conditions (4.5). In this case the velocity, pressure and stream function are represented in terms of Green's functions, namely

$$v^\infty(z_0) = \frac{1}{\pi}\int_{\mathscr{B}^+}\left[K_v\,(z_0,z)\,f(z) + K_v\left(z_0,z^*\right)\,f(z)^*\right]\,\mathrm{d}s \ ,$$

$$p^\infty(z_0) = C^\infty + \frac{2\mu}{\pi}\int_{\mathscr{B}^+}\mathrm{Re}\left[K_p\,(z_0,z)\,f(z)\right]\,\mathrm{d}s \ ,$$

$$\psi^\infty(z_0) = \frac{1}{\pi}\int_{\mathscr{B}^+}\mathrm{Im}\left[K_\psi\,(z_0,z)\,f(z)\right]\,\mathrm{d}s \ ,$$

where $f(z)$ is the unknown density defined on $\mathscr{B}^+$ which is that part of the rigid boundary $\mathscr{B}$ which belongs to the first quadrant $\{x \geqslant 0, y \geqslant 0\}$. The kernels are given by

$$K_v(z_0, z) = \log\left|\frac{z_0 + z}{z_0 - z}\right| + \frac{z_0 z - z_0^* z^*}{(z_0^*)^2 - z^2},$$

$$K_p(z_0, z) = \frac{4\left[|z_0|^4 - \mathrm{Re}\,(z_0^2)\, z^2\right]}{z\left[|z_0|^4 - 2\,\mathrm{Re}\,(z_0^2)\, z^2 + z^4\right]},$$

$$K_\psi(z_0, z) = (z_0^* - z^*)\log\left|\frac{z_0 + z}{z_0 - z}\right| + (z_0 - z^*)\log\left|\frac{z_0^* + z}{z_0^* - z}\right| + 2z^*\log\left|\frac{z_0 + z}{z_0^* - z}\right|.$$

The constant C^∞ is equal to the pressure at the mill centre, which is undetermined in incompressible fluid mechanics.

It is straightforward to check that the local flow field about the centre of the mill is calculated as

$$\psi^\infty(z) = -\tfrac{1}{2}\mathrm{Im}\left[\left(G + G_1|z|^2 + G_2 z^2\right) z^2\right] + O\left(|z|^6\right),$$

where

$$G = \frac{4}{\pi}\int_{\mathscr{B}^+} \mathrm{Re}\,(z^*/z)\ \mathrm{Re}\left[f(z)/z\right] ds,$$

$$G_1 = -\frac{4}{3\pi}\int_{\mathscr{B}^+} \mathrm{Re}\left[f(z)/z^3\right] ds,$$

$$G_2 = \frac{1}{3\pi}\int_{\mathscr{B}^+} \mathrm{Re}\left[\left(\frac{3z^*}{z^4} + \frac{1}{(z^*)^3}\right) f(z)\right] ds.$$

Note that $G_2 = 0$ due to (4.5), which is also confirmed numerically. In particular, the truncated velocity field, pressure, stress and stream functions are given by

$$V^\infty(z) = G(x - \mathrm{i}y) + G_1\left[x(x^2 + 3y^2) - \mathrm{i}\,y(3x^2 + y^2)\right], \tag{4.6a}$$

$$P^\infty(z) = C^\infty + 6\mu G_1(x^2 - y^2), \tag{4.6b}$$

$$\Phi^\infty(z) = -\frac{C^\infty}{4\mu}(x^2 + y^2) - \tfrac{1}{2}\left[G + G_1(x^2 + y^2)\right](x^2 - y^2), \tag{4.6c}$$

$$\Psi^\infty(z) = -\left[G + G_1(x^2 + y^2)\right] x\,y. \tag{4.6d}$$

Unlike (2.1), the local pressure (4.6*b*) is not constant. In this connection, there arises the dimensionless constant

$$C_1 = \frac{G_1 L^2}{G},$$

where L is the half-size of the mill side (in Taylor's experiments, $L = 3.8$ cm), which is associated with the local pressure gradient. The sign of C_1 will tell us whether the drop should cusp or burst with increasing strain.

4.3. *Inner solution*

Consider a two-dimensional drop of area $A = \pi R^2$ placed within unbounded fluid with the far-field flow given by (4.6*a*)–(4.6*d*). In this case the stress–stream function at infinity has the expression

$$W^\infty(z) = -\frac{1}{2}\left[\left(G + G_1|z|^2\right) z^2 + \frac{C^\infty}{2\mu}|z|^2\right], \tag{4.7}$$

where C^{∞} is unknown.

Following Taylor (1934), let us introduce the deformation parameter (2.2), capillary number (2.3) and, additionally, the pressure parameter ε given by

$$\varepsilon = \frac{G_1 R^2}{G} \equiv C_1 \left(\frac{R}{L}\right)^2 . \tag{4.8}$$

The inner problem will be solved analytically, using complex-variable techniques. Superscript '$\circ$' indicating the inner solution, will be omitted in the following.

Using the Goursat representation (4.1) and taking advantage of the formula

$$2\frac{\partial w}{\partial z^*} = \frac{\partial z}{\partial s}\left[\frac{\partial \varphi}{\partial s} - \frac{\partial \psi}{\partial n} + \mathrm{i}\left(\frac{\partial \varphi}{\partial n} + \frac{\partial \psi}{\partial s}\right)\right] ,$$

which is merely the definition of the complex partial derivative in the local coordinate system (s, n), the boundary conditions (4.4) take the form (Richardson 1968; Jeong & Moffatt 1992)

$$w_0(z) + z^* w_1(z) = 0 , \quad \mathrm{Im}\left[\frac{\partial z^*}{\partial s} w_1(z)\right] = \frac{\sigma}{4\mu} \quad \text{on } \mathscr{S} , \tag{4.9}$$

which have to be solved in combination with the asymptotic conditions at infinity

$$w_0(z) \sim -\tfrac{1}{2} G z^2 , \quad w_1(z) \sim -\tfrac{1}{2} G_1 z^3 - \frac{C^{\infty}}{4\mu} z \quad \text{as } z \to \infty , \tag{4.10}$$

following from (4.7).

By Riemann's theorem, there exists a conformal mapping of the infinite flow domain $\mathscr{D}^{\circ}$ onto the disc $\mathscr{G} = \{|\zeta| < 1\}$, given by $z = z(\zeta)$. Moreover, this mapping function is unique if one requires that

$$\lim_{\zeta \to 0} [\zeta\, z(\zeta)] > 0 . \tag{4.11}$$

In particular, $z(0) = \infty$. In addition, since the drop is doubly symmetric,

$$-z(-\zeta) = z(\zeta) , \quad z\left(\zeta^*\right)^* = z(\zeta) . \tag{4.12}$$

Let us make the change of variables $z = z(\zeta)$ retaining the same notation for the unknown functions, e.g.

$$w(\zeta) = w_0(\zeta) + z(\zeta)^* w_1(\zeta) .$$

Then the inner problem (4.9) takes the form

$$w_0\left(\mathrm{e}^{\mathrm{i}\vartheta}\right) + z\left(\mathrm{e}^{\mathrm{i}\vartheta}\right)^* w_1\left(\mathrm{e}^{\mathrm{i}\vartheta}\right) = 0 , \tag{4.13a}$$

$$\mathrm{Re}\left[\frac{w_1\left(\mathrm{e}^{\mathrm{i}\vartheta}\right)}{\mathrm{e}^{\mathrm{i}\vartheta} z'\left(\mathrm{e}^{\mathrm{i}\vartheta}\right)}\right] = -\frac{\sigma}{4\mu\left|z'\left(\mathrm{e}^{\mathrm{i}\vartheta}\right)\right|} < 0 , \tag{4.13b}$$

and the asymptotic conditions (4.10) reduce to

$$w_0(\zeta) \sim -\tfrac{1}{2} G z^2(\zeta) \quad \text{as } \zeta \to 0 , \tag{4.14a}$$

$$w_1(\zeta) \sim -\tfrac{1}{2} G_1 z^3(\zeta) - \frac{C^{\infty}}{4\mu} z(\zeta) \quad \text{as } \zeta \to 0 . \tag{4.14b}$$

It is straightforward to check that the Schwartz problem (4.13*b*) and (4.14*b*) has the

unique symmetric solution

$$w_1(\zeta) = -\tfrac{1}{2}G_1 z^3(\zeta) + \frac{\zeta z'(\zeta)}{2\pi}\int_{-\pi}^{\pi}\left\{\tfrac{1}{2}G_1 \operatorname{Re}\left[\frac{z^3(\mathrm{e}^{\mathrm{i}\vartheta})}{\mathrm{e}^{\mathrm{i}\vartheta} z'(\mathrm{e}^{\mathrm{i}\vartheta})}\right] - \frac{\sigma}{4\mu\,|z'(\mathrm{e}^{\mathrm{i}\vartheta})|}\right\}\frac{\mathrm{e}^{\mathrm{i}\vartheta}+\zeta}{\mathrm{e}^{\mathrm{i}\vartheta}-\zeta}\,\mathrm{d}\vartheta\,,$$

which is an analytic function in the disc $\mathscr{G}$ with a triple pole at the origin. In addition, equation (4.13*b*) in combination with the argument principle suggests that $w_1(\zeta)$ has exactly two simple zeros in $\mathscr{G}$, say β_1 and β_2, or just one double zero if β_1 merges with β_2 (Antanovskii 1994*c*). Note that the constant C^∞ is also determined as

$$\begin{aligned} C^\infty &= -4\mu\lim_{\zeta\to 0}\left[\frac{w_1(\zeta)}{z(\zeta)} + \tfrac{1}{2}G_1 z^2(\zeta)\right] \\ &= \frac{1}{2\pi}\int_{-\pi}^{\pi}\left\{2\mu G_1 \operatorname{Re}\left[\frac{z^3(\mathrm{e}^{\mathrm{i}\vartheta})}{\mathrm{e}^{\mathrm{i}\vartheta} z'(\mathrm{e}^{\mathrm{i}\vartheta})}\right] - \frac{\sigma}{|z'(\mathrm{e}^{\mathrm{i}\vartheta})|}\right\}\mathrm{d}\vartheta\,. \end{aligned}$$

Likewise, taking the real part of equation (4.13*a*) and solving the resulting Schwartz problem with the condition (4.14*a*), one obtains

$$w_0(\zeta) = -\tfrac{1}{2}G z^2(\zeta) + \frac{1}{2\pi}\int_{-\pi}^{\pi}\operatorname{Re}\left[\tfrac{1}{2}G z^2(\mathrm{e}^{\mathrm{i}\vartheta}) - z(\mathrm{e}^{\mathrm{i}\vartheta})^* w_1(\mathrm{e}^{\mathrm{i}\vartheta})\right]\frac{\mathrm{e}^{\mathrm{i}\vartheta}+\zeta}{\mathrm{e}^{\mathrm{i}\vartheta}-\zeta}\,\mathrm{d}\vartheta\,,$$

which is analytic in the disc $\mathscr{G}$ with a double pole at the origin.

Furthermore, equation (4.13*a*) suggests that the conformal mapping $z(\zeta)$ can be analytically continued on the whole plane as (Richardson 1968)

$$z(\zeta) = -\,w_0(1/\zeta^*)^*\big/\,w_1(1/\zeta^*)^*\,,\quad |\zeta| > 1\,,$$

from which it is straightforward to check that $z(\zeta)$ must be a rational function, more specifically

$$z(\zeta) = \frac{\alpha_0 + \alpha_1\zeta + \alpha_2\zeta^2}{\zeta\,(1-\beta_1^*\zeta)\,(1-\beta_2^*\zeta)}\,,$$

where $\alpha_0 > 0$ due to the normalization condition (4.11). Indeed, $z(\zeta)$ is defined on the whole complex plane and has exactly three simple poles at $\zeta = 0$, $1/\beta_1^*$ and $1/\beta_2^*$, and vanishes at infinity (Antanovskii 1994*c*). These coefficients are determined from the requirement that the function

$$U(\zeta) = w_0(\zeta) + z(1/\zeta^*)^* w_1(\zeta)$$

has only removable singularities within $\mathscr{G}$. Actually, the function $U(\zeta)$ must be identically zero due to (4.13*a*), which will be satisfied by the above requirement, since the real part of $U(\zeta)$ is already zero. Note that $z(1/\zeta^*)^*$ has two simple poles at $\zeta = \beta_1$ and β_2.

Owing to the symmetry condition (4.12),

$$z(\zeta) = \frac{R(\alpha+\beta\zeta^2)}{\zeta(1-\gamma\zeta^2)}\,, \tag{4.15}$$

where α, β, and γ are dimensionless real coefficients (Antanovskii 1995). The condition for the function $U(\zeta)$ to be regular at the origin immediately gives $\gamma = \varepsilon\alpha\beta$. The remaining singularities at $\zeta = \pm\gamma^{1/2}$ are removed if $w_1(\pm\gamma^{1/2}) = 0$. Rearranging, the

latter reduces to the transcendental equation (Antanovskii 1994*b*, 1995)

$$\lambda = \frac{\beta}{\pi\,\alpha}\int_0^{\pi} \frac{\mathrm{d}\vartheta}{\left|\alpha\,\left(1-3\varepsilon\,\alpha\,\beta\,\mathrm{e}^{\mathrm{i}\vartheta}\right)-\beta\,\mathrm{e}^{\mathrm{i}\vartheta}\,\left(1+\varepsilon\,\alpha\,\beta\,\mathrm{e}^{\mathrm{i}\vartheta}\right)\right|}\,. \tag{4.16}$$

Finally, the coefficient α is discarded from the condition that the drop area is equal to πR^2, which gives

$$\alpha = \left\{\frac{2\left(1+\beta^2\right)}{A_\varepsilon(\beta)+\left[A_\varepsilon^2(\beta)-B_\varepsilon(\beta)\right]^{1/2}}\right\}^{1/2} > 0\,, \tag{4.17}$$

where

$$A_\varepsilon(\beta) = 1-\varepsilon\beta^2\,\left[2(1-\varepsilon)+\varepsilon\,\beta^2\right]\,,$$

$$B_\varepsilon(\beta) = 4\varepsilon^2\,\beta^2\,\left(1+\beta^2\right)\left[3+\varepsilon\,(2+\varepsilon)\,\beta^2\right]\,.$$

Equations (4.16) and (4.17) implicitly determine the conformal mapping in terms of the given parameters λ and ε. Then, using (4.15), the deformation parameter δ is found from the formula

$$\delta \equiv \frac{z(1)+\mathrm{Im}[z(\mathrm{i})]}{z(1)-\mathrm{Im}[z(\mathrm{i})]} = \frac{\beta\,\left(1+\varepsilon\,\alpha^2\right)}{\alpha\,\left(1+\varepsilon\,\beta^2\right)}\,.$$

The tip curvature of the drop endpoints is similarly calculated:

$$-\kappa \equiv \frac{z''(1)+z'(1)}{z'(1)^2} = \frac{(1-\varepsilon\,\alpha\,\beta)\left[\alpha+\beta-2\varepsilon\,\alpha\,\beta\,(\alpha-3\beta)+\varepsilon^2\,\alpha^2\,\beta^2\,(9\alpha+\beta)\right]}{R\,\left[\alpha-\beta-\varepsilon\,\alpha\,\beta\,(3\alpha+\beta)\right]^2}\,.$$

Note that, for pure straining flow ($\varepsilon = 0$), equations (4.16) and (4.17) reduce to the single equation (Richardson 1968)

$$\lambda = \frac{2\delta}{\pi}\left(\frac{1-\delta}{1+\delta}\right)^{1/2} K\left[\frac{2\delta^{1/2}}{1+\delta}\right] \equiv \frac{2\delta}{\pi}\left(1-\delta^2\right)^{1/2} K[\delta]\,,\quad 0 \leqslant \delta < 1\,, \tag{4.18}$$

where K is the complete elliptic integral of the first kind,

$$K[m] = \int_0^{\pi/2} \frac{\mathrm{d}\vartheta}{\left(1-m^2\,\sin^2\vartheta\right)^{1/2}}\,.$$

In this case, since (4.15) becomes Joukowski's function, the drop assumes an elliptical cross-section the tip curvature of which is expressed in terms of δ as

$$-\kappa = \frac{1}{R}\left(\frac{1+\delta}{1-\delta}\right)^{3/2}\,. \tag{4.19}$$

Using the well-known asymptotic properties of $K[m]$ as $m \to 1$, it is straightforward to check that

$$\lambda \approx \frac{2\delta}{\pi}\left(\frac{1-\delta}{1+\delta}\right)^{1/2} \log\left(4\,\frac{1+\delta}{1-\delta}\right) \quad \text{as } \delta \to 1\,,$$

which appears to fit equation (4.18) quite well for all δ.

5. Results and discussion

Numerical simulations of the outer solution are carried out exactly for Taylor's mill described in §2, using 300 linear boundary elements. The integral terms over the

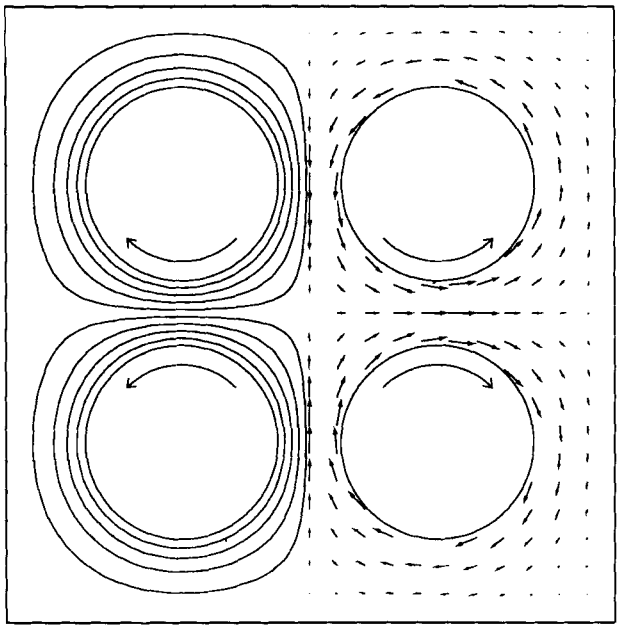

FIGURE 2. Stream lines and velocity field for viscous flow in Taylor's four-roller mill. The computations suggest that $C_0 = 4.79$ and $C_1 = 2.54$.

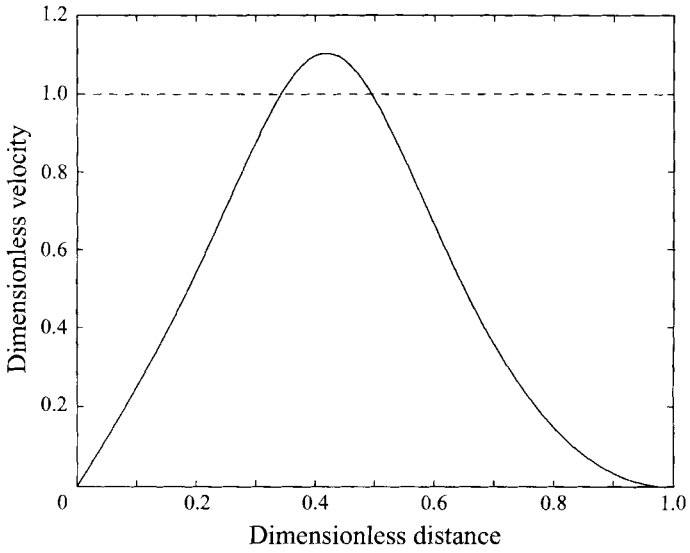

FIGURE 3. Dimensionless velocity, $v_x(x)/V$, on the x-axis versus dimensionless distance, x/L.

boundary elements are evaluated by the fourth-order Gaussian quadrature formula. When the observation point is right on the source-point element, the leading-order singularity is computed analytically and the remainder numerically (Pozrikidis 1992).

The outer-flow pattern in the mill is plotted in figure 2. The computations suggest that $C_1 = 2.54$, and $C_0 = 4.79$ which is quite close to Taylor's $C_0 = 5.1$. It is important to emphasize that $C_1 > 0$. If it were negative, say for another mill configuration, an inviscid drop would burst with increasing strain rather than cusp. The dimensionless

x_1 (cm)	x_2 (cm)	$(t_2 - t_1)$ (s)	
		Measured	Computed
0.5	1.0	7.0	6.4
1.0	1.5	3.9	3.5
1.5	2.0	2.7	3.1
2.0	2.5	2.0	4.9

TABLE 1. Dimensional displacement and time for a particle to pass along the x-axis from x_1 to x_2 in Taylor's four-roller mill at $T = 48.7$ s.

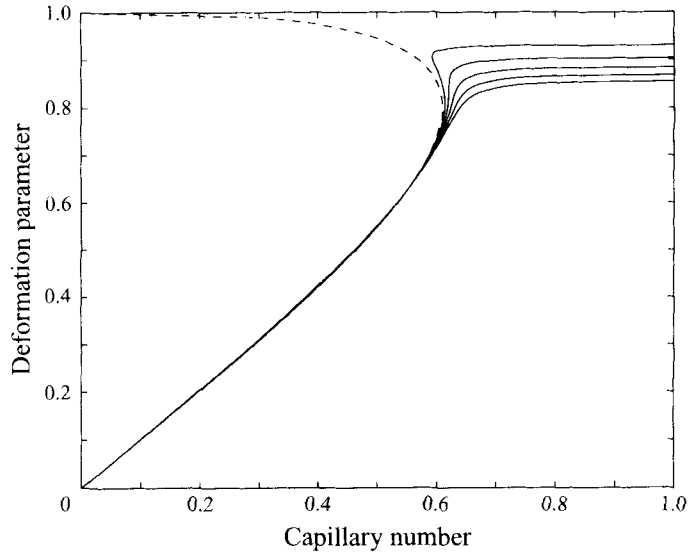

FIGURE 4. Response diagrams (δ versus λ) for $\varepsilon = 0$ (broken line), 0.002, 0.004, 0.006, 0.008 and 0.01 (solid lines), respectively.

velocity v_x/V on the positive x-axis as a function of x/L is given in figure 3, where V is the rollers' linear velocity and L is the half-size of the mill side. Note that, in Taylor's experiments, $L = 3.8$ cm and $V = 0.1542\ \text{cm s}^{-1}$ at $T = 48.7$ s. The calculated times of passages of a particle on the x-axis compared to those measured by Taylor (1934) are presented in table 1. The discrepancy between the measured and computed values in rows 1 and 2 can be explained by the fact that the actual flow set up by Taylor is three-dimensional due to the presence of the front and rear sides of the mill, which reduce the flow field. However, rows 3 and 4 show that, far from the mill centre, the measured flow is even faster than the computed one. Plausibly, this is also caused by a three-dimensional effect (for example, the observed particles flow at different speeds in different planes parallel to the front side of the mill).

The plots of δ and $R|\kappa|$ versus λ are given for some values of ε in figures 4 and 5, respectively. Note that $\delta \approx \lambda$ for small λ (all the curves in figure 4 have tangent line $\delta = \lambda$ at $\delta = 0$). For a three-dimensional drop, this fact was theoretically predicted and experimentally verified by Taylor (1932, 1934). Functions (4.18) and (4.19) are shown by the broken lines. Notice a maximum value $\lambda_* \approx 0.61$ of the function (4.18) at $\delta_* \approx 0.8$, which is close to Taylor's critical value 0.65 at which a sudden transition to a pointed drop occurred. A similar response diagram was plotted by Buckmaster

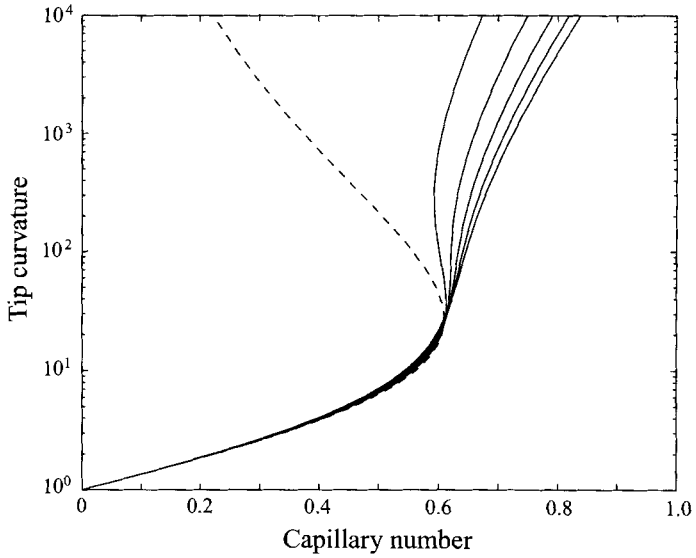

FIGURE 5. Dimensionless tip curvature, $R|\kappa|$, versus λ for $\varepsilon = 0$ (broken line), 0.002, 0.004, 0.006, 0.008 and 0.01, respectively.

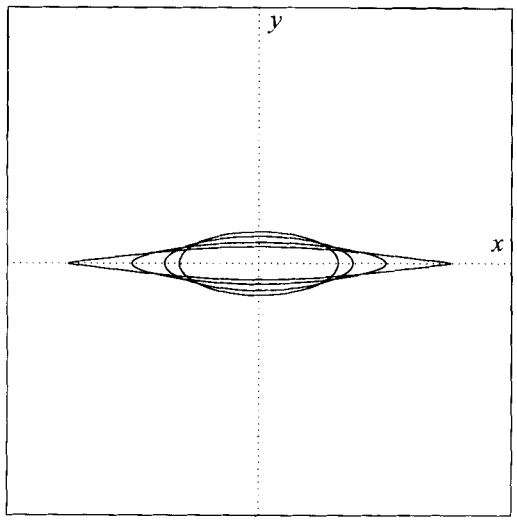

FIGURE 6. Increasingly elongated shapes of a drop of radius $R = 0.25$ cm ($\varepsilon = 0.01$) in Taylor's flow at $\lambda = 0.4$, 0.5, 0.6 and 0.7, respectively.

& Flaherty (1973) for a drop of the same viscosity as the exterior fluid. Thus, beyond λ_*, no steady solution with $\varepsilon = 0$ exists, whereas two possible solutions exist for $\lambda < \lambda_*$, one of which becomes unstable with greater δ (Buckmaster & Flaherty 1973; Antanovskii 1994*b*). For $\varepsilon > 0$, the response diagrams have horizontal asymptotes as λ tends to infinity. Hence, the drop survives for all strains and becomes cusped when $\lambda \to \infty$ as is suggested by figure 5. In particular, it shows exponential growth of κ with increasing λ, which is similar to the result by Jeong & Moffatt (1992).

Furthermore, for $\varepsilon \geqslant \varepsilon_* \approx 0.004$, the drop deformation δ is a one-to-one function of the capillary number λ. Note that, for Taylor's mill, the critical pressure parameter

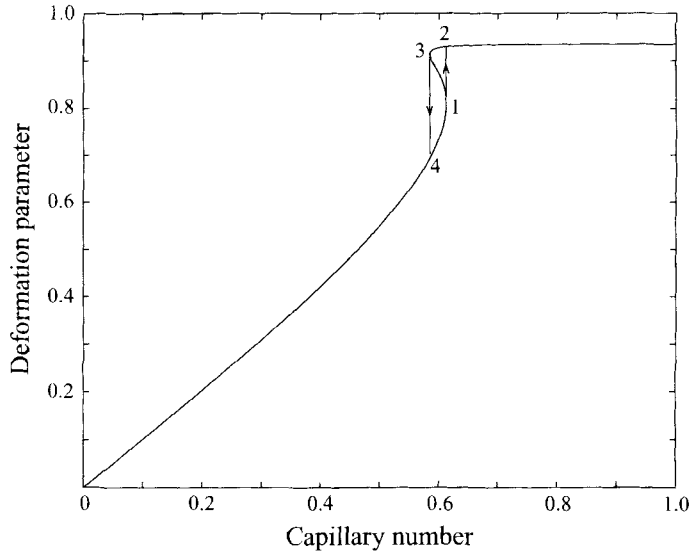

FIGURE 7. Response diagram (δ versus λ) for a drop of radius $R = 0.1$ cm ($\varepsilon = 0.00174$). The arrows indicate transition from unstable to stable configurations.

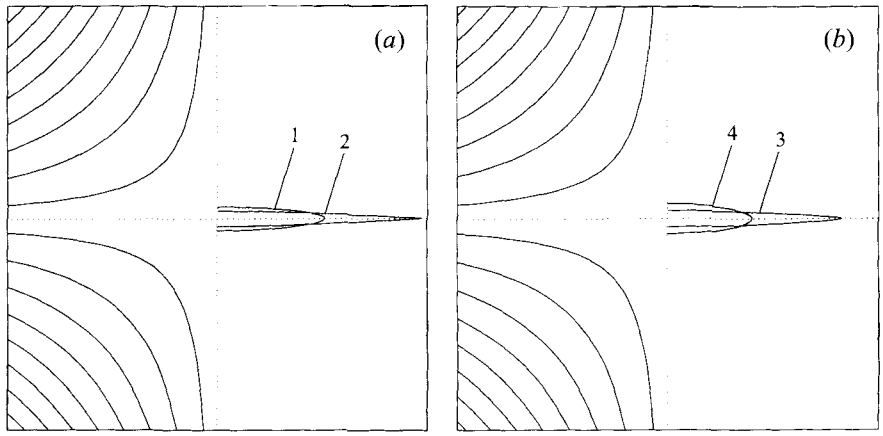

FIGURE 8. (*a*) Stream lines of the local outer flow ($\lambda = 0.613$), and the shapes of a drop of radius $R = 0.1$ cm ($\varepsilon = 0.00176$) corresponding to states 1 and 2 shown in figure 7. (*b*) Stream lines of the local outer flow ($\lambda = 0.585$), and the shapes of a drop of radius $R = 0.1$ cm ($\varepsilon = 0.00174$) corresponding to states 3 and 4 shown in figure 7.

ε_* corresponds to the drop radius $R_* = 0.15$ cm. The shapes of a fairly large drop of radius $R = 0.25$ cm, which roughly corresponds to $\varepsilon = 0.01$, are depicted in figure 6 for some values of λ. It is seen that these have remarkable similarities with the three-dimensional drops documented by Taylor (1934) and Rumscheidt & Mason (1961). For $0 < \varepsilon < \varepsilon_*$, a multi-valued dependence of δ on λ occurs. In particular, for a certain interval of capillary numbers, three possible solutions, say δ_1, δ_2, δ_3 ($\delta_1 < \delta_2 < \delta_3$), exist. It is conceivable that the solution δ_2 described by the decreasing dependence of λ on δ is unstable. Therefore, with increasing λ, the solution δ_1 will merge with δ_2 at a critical λ and then a transition to δ_3 must occur, and *vice versa*, with decreasing λ, the solution δ_3 will merge with δ_2 at another critical value of λ

and a transition to δ_1 will be seen. These bifurcations are indicated by the arrows in figure 7, which form a typical hysteresial loop. The shapes of the drop at the critical capillary numbers along with the stream lines of the critical flows, plotted with the difference $3GR^2$ in the stream function, are shown in figure 8. It is seen that the drop shapes differ significantly. This effect can be identified with the sudden transition of a rounded drop to a pointed one.

6. Concluding remarks

The results obtained can be roughly summed up as follows. The two-dimensional flow in Taylor's four-roller mill with no drop effect is computed numerically, using a boundary-element method. Then the local structure of that flow at the mill centre, where the drop is positioned, is used to complete the inner problem for the drop behaviour. It is shown that this flow distorts the drop until it develops two cusps in the capillary interface with increasing strain. Note that the cusps are apparent, because the conformal mapping (4.15) is analytic on the disc boundary $\partial\mathscr{G}$, and hence the drop interface is always an analytic curve, though its curvature can reach extremely high magnitudes with increasing strain.

It is worth emphasising that the cusps are formed at those stagnation points of the drop interface where the inner flow is convergent (Jeong & Moffatt 1992). So, the effect of surfactants which can be convected towards those points in diminishing the surface tension, can facilitate the cusp formation. This effect can be studied analytically as is done in Antanovskii (1994*a*).

Response diagrams showing the drop deformation versus capillary number are plotted, which demonstrate that, for the pressure parameter ε beyond a critical value ε_*, or equivalently, for the drop size greater than a critical one, a unique solution exists for all capillary numbers. Otherwise, multiple solutions occur in a certain interval of λ, which may result in a hysteresial behaviour of the drop. The study of this phenomenon will be the subject of a separate paper. In this context it is worth noting that a time-evolving drop can be described by the rational conformal mapping of the same form (4.15) but with time-dependent coefficients.

The author is grateful to Professors A. Acrivos, R. H. J. Grimshaw, D. D. Joseph and H. K. Moffatt for helpful discussion and stimulation of this work. The comments of anonymous referees are greatly appreciated.

REFERENCES

Acrivos, A. & Lo, T. S. 1978 Deformation and breakup of a single slender drop in an extensional flow. *J. Fluid Mech.* **86**, 641–672.

Antanovskii, L. K. 1994*a* Influence of surfactants on a creeping free-boundary flow induced by two counter-rotating horizontal thin cylinders. *Eur. J. Mech.* B/*Fluids* **13**, 73–92.

Antanovskii, L. K. 1994*b* Quasi-steady deformation of a two-dimensional bubble placed within a potential viscous flow. *Meccanica – J. Ital. Assoc. Theor. Appl. Mech.* **29**, 27–42.

Antanovskii, L. K. 1994*c* A plane inviscid incompressible bubble placed within a creeping viscous flow: formation of a cusped bubble. *Eur. J. Mech.* B/*Fluids* **13**, 491–509.

Antanovskii, L. K. 1995 Mathematical modelling of formation of a pointed drop in a four-roll mill. In *Proc. 3rd Caribbean Congr. on Fluid Dynamics and the 3rd Latin–American Symp. on Fluid Mechanics, Caracas, Venezuela, 2–9 Feb. 1995* (ed. J. J. Manzano-Ruíz, S. Zarea, A. Tremante, E. Guevara & R. García), vol. 1, pp. 1–6, Universidad Simón Bolívar.

Buckmaster, J. D. 1972 Pointed bubbles in slow viscous flow. *J. Fluid Mech.* **55**, 385–400.

BUCKMASTER, J. D. 1973 The bursting of pointed drops in slow viscous flow. *Trans ASME J. Appl. Mech.* E: **40**, 18–24.

BUCKMASTER, J. D. & FLAHERTY, J. E. 1973 The bursting of two-dimensional drops in slow viscous flow. *J. Fluid Mech.* **60**, 625–639.

HINCH, E. J. & ACRIVOS, A. 1979 Steady long slender droplets in two-dimensional straining motion. *J. Fluid Mech.* **91**, 401–414.

HOPPER, R. W. 1990 Plane Stokes flow driven by capillarity on a free surface. *J. Fluid Mech.* **213**, 349–375.

HOPPER, R. W. 1991 Plane Stokes flow driven by capillarity on a free surface. Part 2. Further developments. *J. Fluid Mech.* **230**, 355–364.

HOPPER, R. W. 1992 Stokes flow of a cylinder and a half-space driven by capillarity. *J. Fluid Mech.* **243**, 171–181.

HOPPER, R. W. 1993 Capillarity-driven plane Stokes flow exterior to a parabola. *Q. J. Mech. Appl. Maths* **46**, 193–210.

HROMADKA II, T. V. & LAI, C. 1987 *The Complex Variable Boundary Element Method in Engineering Analysis.* Springer.

JEONG, J. T. & MOFFATT, H. K. 1992 Free surface cusps associated with flow at low Reynolds number. *J. Fluid Mech.* **241**, 1–22.

JOSEPH, D. D., NELSON, J., RENARDY, M. & RENARDY, Y. 1991 Two-dimensional cusped interfaces. *J. Fluid Mech.* **223**, 383–409.

LANGLOIS, W. E. 1964 *Slow Viscous Flow.* Macmillan.

LIU, Y. J., LIAO, T. Y. & JOSEPH, D. D. 1995 Two-dimensional cusp at the trailing edge of an air bubble rising in a viscoelastic liquid. *J. Fluid Mech.* **304**, 321–342.

MOFFATT, H. K. 1977 Behaviour of a viscous film on the outer surface of a rotating cylinder. *J. Mécanique* **16**, 651–673.

POZRIKIDIS, C. 1992 *Boundary Integral and Singularity Methods for Linearized Viscous Flow.* Cambridge University Press.

RICHARDSON, S. 1968 Two-dimensional bubbles in slow viscous flows. *J. Fluid Mech.* **33**, 475–493.

RICHARDSON, S. 1973 Two-dimensional bubbles in slow viscous flows. Part 2. *J. Fluid Mech.* **58**, 115–127.

RICHARDSON, S. 1992 Two-dimensional slow viscous flows with time-dependent free boundaries driven by surface tension. *Eur. J. Appl. Maths* **3**, 193–207.

RUMSCHEIDT, F. D. & MASON, S. G. 1961 Particle motion in sheared suspensions. XII. Deformation and burst of liquid drops in shear and hyperbolic flow. *J. Colloid Sci.* **16**, 238–261.

SHERWOOD, J. D. 1981 Spindle-shaped drops in a viscous extensional flow. *Math. Proc. Camb. Phil. Soc.* **90**, 529–536.

SHERWOOD, J. D. 1984 Tip streaming from slender drops in a nonlinear extensional flow. *J. Fluid Mech.* **144**, 281–295.

STONE, H. A. 1994 Dynamics of drop deformation and breakup in viscous fluids. *Ann. Rev. Fluid Mech.* **26**, 65–102.

TANVEER, S. & VASCONCELOS, G. L. 1995 Time-evolving bubbles in two-dimensional Stokes flow. *J. Fluid Mech.* **301**, 325–344.

TAYLOR, G. I. 1932 The viscosity of a fluid containing small drops of another fluid. *Proc. R. Soc. Lond.* A **138**, 41–48.

TAYLOR, G. I. 1934 The formation of emulsions in definable fields of flow. *Proc. R. Soc. Lond.* A **146**, 501–523.

YOUNGREN, G. K. & ACRIVOS, A. 1976 On the shape of a gas bubble in a viscous extensional flow. *J. Fluid Mech.* **76**, 433–442.